Precision Terrain Mapping Using Large Baseline Interferometry[1]

Neil Carender, J. Craig Dwyer, James Abshier, Eric Cowen, and Brent Howlett
Veridian ERIM International, Inc.
P.O. Box 134008
Ann Arbor, MI 48113-4008
734-994-1200
carender@erim-int.com

Abstract—Veridian ERIM International, with support from the US Air Force and the Defense Advanced Research Projects Agency Tactical Technology Office (DARPA/TTO), has developed an airborne X-band SAR system capable of collecting single-pass interferometric SAR data with cross-track baselines of 7.5 m, 15 m, and 30 m. SAR data have been collected over several sites with varying terrain and groundcover type. These data have been formed into 1-foot resolution imagery and interferometric processing has produced digital elevation data with post spacings of 1 m. The resulting elevation data have been compared with LIDAR elevation data in order to estimate the accuracy of the SAR elevation measurements. SAR elevation data with accuracy approaching the draft Level 5 specification for precision elevation data have been produced.

TABLE OF CONTENTS

1. INTRODUCTION

Single-pass interferometric synthetic aperture radar (IFSAR) systems have demonstrated the capability to rapidly collect and generate terrain elevation data with 10 m post spacings, absolute LE90 < 5 m, and random LE90 errors < 2 m [1]. However, emerging applications require precision terrain data with post spacings of 1 m to 3 m, and random LE90 errors < 1 m.

This paper presents the initial results obtained from a large-baseline, single-pass IFSAR terrain mapping system. The emphasis of the work is on methods to produce precision terrain data satisfying the aforementioned post spacings and random error requirements. The test data were collected using an X-band SAR with a horizontal baseline of 7.5 m to 30 m. For the collection parameters used, these baselines correspond to differential grazing angles of 0.03° to 0.2° and interferometer ambiguity heights of 3 m to 25 m.

The remainder of this paper is organized as follows. Section 2.0 presents a brief description of the technical approach and motivation for large-baseline IFSAR mapping. Section 3.0 describes the large-baseline IFSAR sensor used to collect the test data. The interferometric SAR data processing is described in Section 4.0. Example results including a comparison against LIDAR ground truth are presented in Section 5.0. Section 6.0 presents a summary of the results obtained and our conclusions.

2. TECHNICAL APPROACH

Random height measurement errors due to phase noise in an interferometric SAR system can be modeled by

$$\sigma_h = \frac{\lambda \cos\beta}{2n\pi} \cdot \frac{1}{\Delta\beta} \cdot \sigma_\phi \qquad (1)$$

where σ_h is the height measurement error, λ is the wavelength corresponding to the radar center frequency, β is the grazing angle (complement of the incidence angle), $\Delta\beta$ is the differential grazing angle between the two phase centers, n=1 for bistatic mode collection and n=2 for monostatic mode collection (these modes are described in Section 3.), and σ_ϕ is the system phase noise.

For a fixed level of phase noise, increasing the differential grazing angle, $\Delta\beta$, will reduce the random height measurement errors. Unfortunately σ_ϕ is a function of $\Delta\beta$, and several other radar system parameters. Increasing the differential grazing angle increases the phase noise due to

[1] 0-7803-5846-5/00/$10.00 © 2000 IEEE

baseline decorrelation. Increasing the baseline also decreases the interferometer ambiguity distance, making phase unwrapping more difficult. Numerous phenomenological effects cause additional decorrelation, and thus increase the phase noise and random height measurement error. In addition to these effects, there are difficult phase center motion measurement and baseline determination issues associated with increasing the baseline.

Two-pass collections can be used to achieve the long baselines, but are subject to potentially severe temporal decorrelation.

3. Description of Large Baseline IFSAR Sensor

The large-baseline IFSAR data were collected with the ERIM International Data Collection System (DCS), a Convair CV-580 aircraft equipped with a flexible radar system used for experimental SAR data collections. The key parameters of the DCS system are given in Table 1.

Figure 1 shows a block diagram of the data collection system. The long-baseline IFSAR configuration of the DCS has 3 radar antennas: one in each wingtip and one in the belly radome. Only two of the three phase centers are used on any given pass. The two active phase centers are selected using the RF switch chassis, which is connected to the

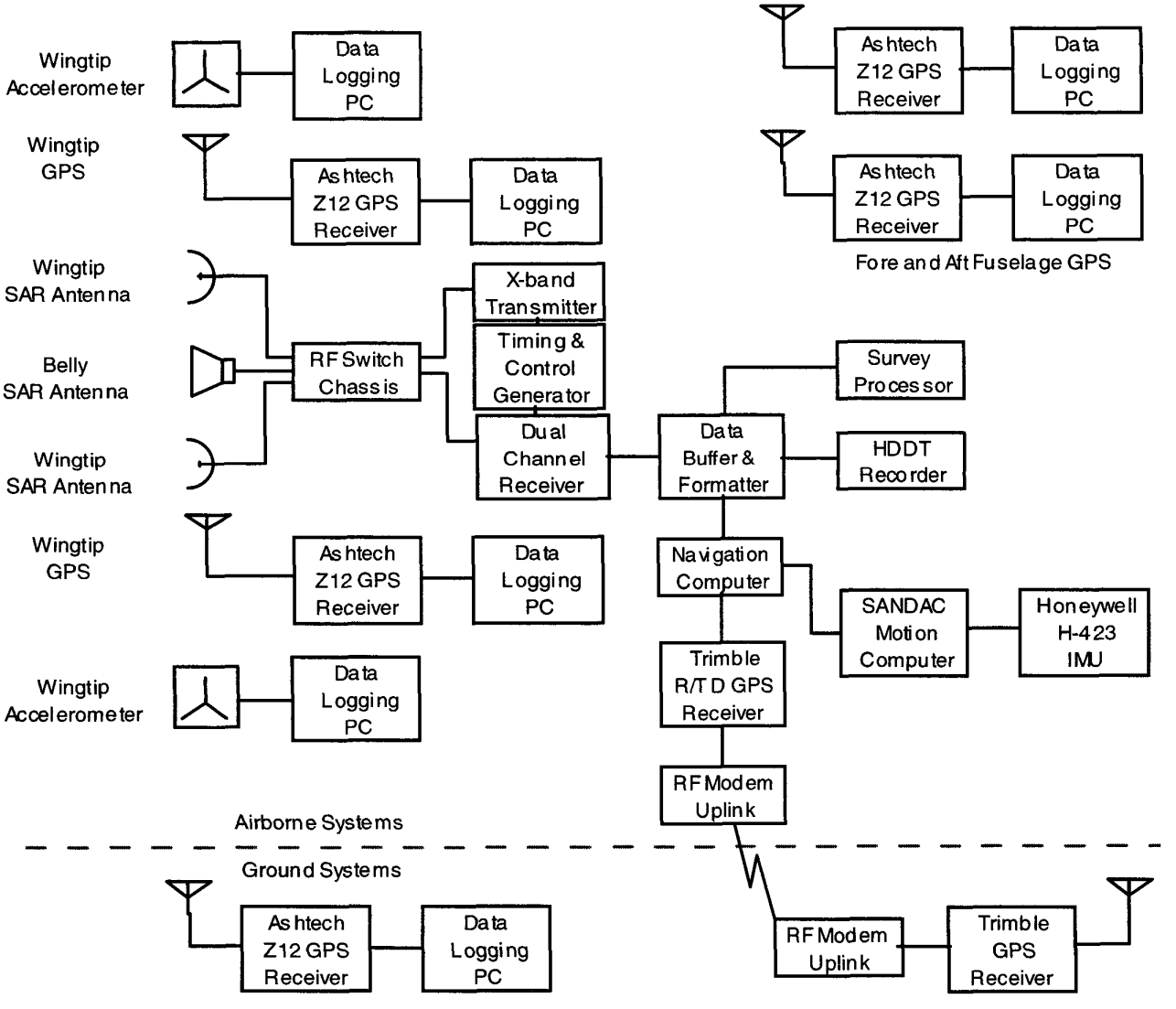

Figure 1: Block diagram of the DCS long baseline interferometric SAR system.

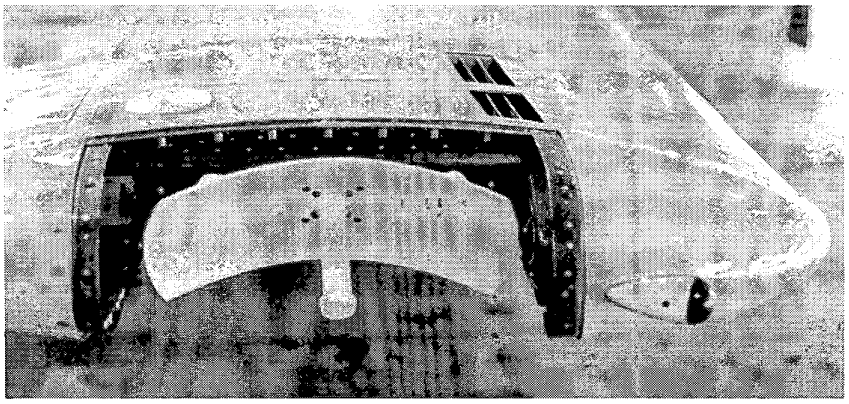

Figure 2: Photograph of the wingtip reflector antenna. The dual-frequency antenna for the wingtip GPS sensor is visible on the upper wing surface, just aft (left) of the radar antenna phase center.

antennas with waveguide. A 600 MHz linear FM (chirp) waveform is digitally synthesized and transmitted, yielding 30 cm range resolution in the slant plane. The received signal is mixed with a second chirp before digitization. A dual-channel receiver enables two phase centers to be collected and recorded simultaneously.

Center Frequency	9.68 GHz
Range Resolution	30 cm
Range Swath (Slant Plane)	455 m
Maximum Altitude	7620 m
Nominal Ground Speed	100 m/sec
PRI per Channel	1024 μsec
PRI Interleaving	2
Simultaneous Channels	2
Total Number of Channels	4

Table 1: SAR Parameters of the Data Collection System

Sensor platform position, attitude, and rotational motion is measured using a Honeywell H-423 Inertial Measurement Unit (IMU). Position measurements are augmented by a Trimble differential GPS system which includes an airborne GPS receiver along with a ground-based GPS receiver. The ground based GPS receiver is normally located at an accurately surveyed position. Differential GPS corrections are uplinked to the airborne receiver via a RF modem. When collecting in spotlight mode, the motion compensation computer provides real-time antenna pointing and stabilization commands to the belly antenna pedestal, derived from the aircraft position and attitude data.

The DCS records the wideband SAR phase history and auxiliary data on high density tape for ground-based image formation. The auxiliary data include navigation data from the IMU and radar system parameters such as the range gate setting and the RMS signal level.

The belly antenna is a lens-corrected horn with 29 dB gain

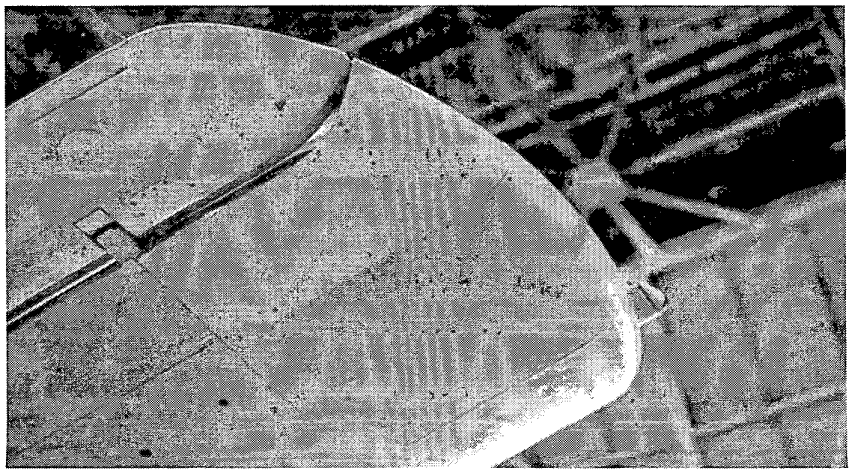

Figure 3: Wingtip SAR antenna with radome in-place.

and a 6° by 6° beamwidth. This antenna is fully polarimetric and is mounted on a motorized pedestal that is controlled by the SAR control computer. This antenna can be adjusted in azimuth to achieve squint angles of +/- 45° and can be adjusted in elevation to achieve depression angles from 30° to 90° (where 90° is looking straight down below the aircraft). The belly-antenna was pointed at fixed azimuth and elevation angle to match the pointing of the wingtip antennas.

Each wingtip contains a 5 inch focal length parabolic reflector with 24 dB of gain covered by a form-fitting radome. Figure 2 shows the wingtip antenna with the radome removed. The radar antenna reflector has been cropped so the antenna can fit (and rotate) within a 6 inch diameter cylindrical volume inside the radome (Figure 3). The wingtip antennas have a 6° azimuth beamwidth and a 14° elevation beamwidth and have fixed azimuth mounts set to broadside. Each tip antenna can be adjusted in elevation to look straight out from the aircraft (horizontal aim, 0° depression angle) down through vertical (90° depression angle) to looking back under the aircraft (30° depression angle). The wingtip antennas are driven by waveguide runs from the radar equipment rack in the main aircraft cabin out through the leading edges of the wings to the wing tips. A rotary waveguide joint at the tip allows the antenna elevation angle to be adjusted. The dual-frequency antenna for the wingtip GPS sensor is visible on the upper wing surface just aft (left) of the radar antenna phase center in Figure 2.

The DCS has two modes utilizing different antenna combinations. The belly-wing mode utilizes the belly antenna and one wingtip antenna (either left or right). The wing-wing mode utilizes the two wingtip antennas. In both modes, the two antennas alternately transmit pulses (ping-pong style), but both antennas receive every pulse, i.e. both monostatic and bistatic data are collected. The monostatic channel data is transmitted and received by the same antenna. There are two monostatic channels; one for each physical phase center. The bistatic channel data is transmitted and received by different antennas. There are two bistatic channels which both have an effective phase center located midway between the transmit and receive antennas. Thus, the two bistatic channels have a common effective phase center location, and only one additional interferometric baseline can be formed. The antennas are fixed in azimuth at broadside and stripmap data is collected. When the two wingtip antennas are used, the system has approximately a 30 m cross-track baseline, and either a 30 m or 15 m interferometric baseline can be processed (depending on whether two monostatic or a monostatic-bistatic pair of channels are processed and interfered). When the belly and wingtip antennas are used, the system has a 15 m physical baseline, and either a 15 m or 7.5 m interferometric baseline can be processed (again depending on channels processed).

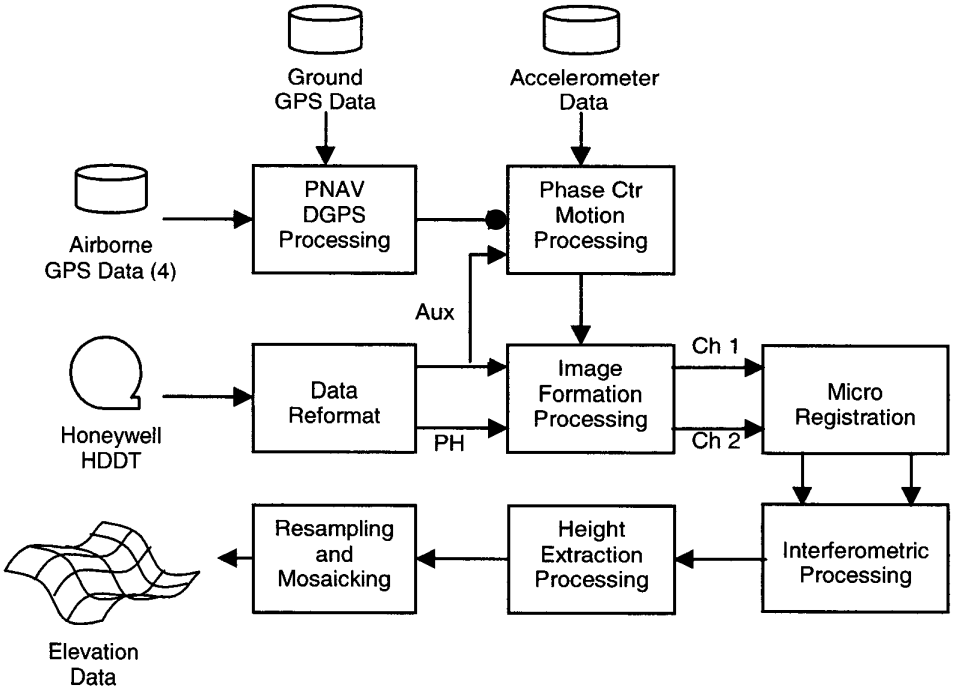

Figure 4: Block diagram of interferometric processing.

Motion measurement and compensation presents a challenge due to the flexible nature of the wing that provides the structure for the interferometer baseline. Wing flexure prevents the fuselage mounted IMU from measuring total wingtip motion using the IMU inertial measurements and lever arm corrections. The motion compensation approach uses a vertically mounted accelerometer to measure high frequency wingtip motion and a wingtip-mounted GPS antenna to measure low frequency motion. The GPS data is differentially corrected using a ground reference DGPS receiver placed near the operational area. The wingtip DGPS and accelerometer data are combined in a Kalman filter to provide the vertical component of the wingtip radar antenna trajectory.

The motion compensation approach assumes that the body lateral components of wing flexure are negligible, i.e. all flexure is perpendicular to the nominal plane of the wing. High frequency motion measurement in the horizontal plane is provided by the existing IMU and corrected for the horizontal components of lever arm to the wingtip radar antenna. This IMU solution has been filtered by DGPS to remove position, velocity, and acceleration biases during the line-up portion of the pass prior to mapping. The GTM motion compensation approach allows the use of the horizontal components of the wingtip DGPS solution to apply a low frequency correction to the lever arm corrected high frequency IMU horizontal data.

Three trajectories are provided to the image formation processor. The two active phase center trajectories are created as described above. The third trajectory is the virtual bistatic phase center located at the midpoint between the two physical (monostatic) phase centers.

4. INTERFEROMETRIC DATA PROCESSING

A block diagram of the interferometric processing flow for the long-baseline IFSAR system is illustrated in Figure 4. Initially, the airborne and ground GPS data are processed using Ashtech's PNAV software to create 5 Hz differential GPS data. In parallel, the High Density Data Tape (HDDT) containing the phase history data and IMU auxiliary data is unloaded and the data are reformatted for image formation processing. The phase-center motion-processing step accepts the 50 Hz wingtip accelerometer data, the 5 Hz DGPS solutions, and the IMU auxiliary data and generates three phase-center motion solutions. Two of the solutions are for the active physical phase centers being used to form the interferometer. The third solution is for the virtual bistatic phase center that is located midway between the two antenna phase centers.

After generation of the motion solutions, the phase history data, along with the motion solution and other auxiliary data are processed to form complex imagery for each channel of

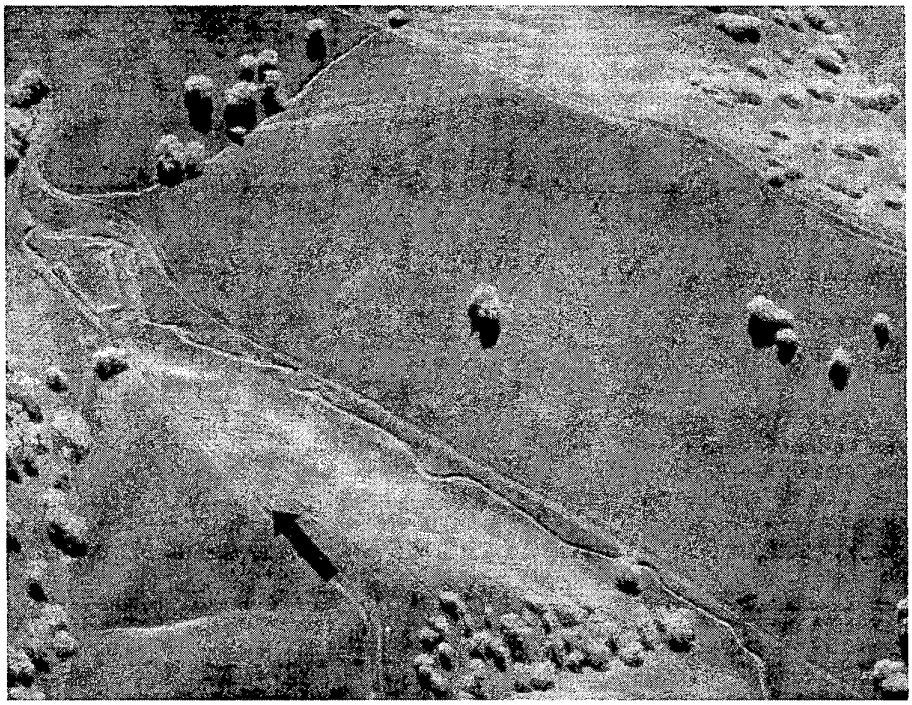

Figure 5: SAR magnitude image of a portion of the Camp Roberts test site. The SAR image resolution is 1 foot. The blue arrow indicates the position and point of view of a photograph of the test site shown in Figure 6.

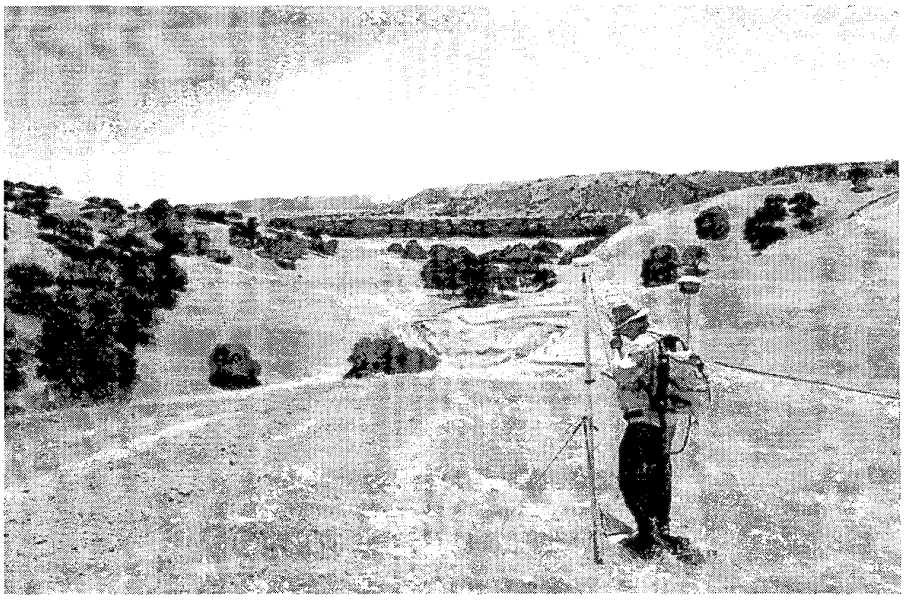

Figure 6: Photograph of the Camp Roberts test site showing the general terrain and ground cover characteristics. One of the corner reflectors used for ground control is shown being surveyed using differential GPS.

data. The image data are micro-registered prior to formation of the interferogram. The micro-registration processing removes any spatially variant mis-registration due to terrain height variations. This step is unnecessary for short baseline systems, but is essential to achieve high correlation levels with a large interferometric baseline. The interferogram is converted to a height map using baseline and collection geometry data. Finally, the height data are resampled (and mosaicked, if multiple patches are being combined) into the desired output product map projection, e.g. UTM.

5. EXAMPLE RESULTS

A 1-foot resolution SAR magnitude image from aircraft pass GTM0211 over the Camp Roberts test site is shown in Figure 5. The image shown is one of a pair of images used for IFSAR terrain measurement. The test area consists of rolling grassy hills with scattered valley oak trees. Figure 6 shows a photograph of the site taken from the position and point of view indicated by the blue arrow in Figure 5. One of the corner reflectors used for ground control is shown being surveyed using differential GPS. Note the trails and dry streambed visible in Figures 5 and 6 for comparison with the corresponding features in the interferogram and the elevation model (shown in Figure 7 and Figure 9, respectively).

Figure 7 shows the interferogram generated from the image in Figure 5 and its interferometric pair. The image pair processed form a 7.5 m effective baseline with a resulting vertical ambiguity height (the height change corresponding to one light-to-dark phase fringe) of approximately 18 m. Note the clearly visible trails and dry stream bed, and the fringe pattern around the scattered trees.

An example of the long-baseline IFSAR elevation data is illustrated in Figure 8, which shows a shaded surface rendering of the IFSAR elevation data (left) along with similar rendering of the LIDAR ground truth data. The IFSAR data is a mosaic of four IFSAR image pairs from two passes, GTM0211 and GTM0206. The ground truth elevation measurements were produced using a FLI-MAP laser detection and ranging (LIDAR) system operated by John Chance and Associates of Lafayette, LA under contract to the US Army Corps of Engineers Topographic Engineering Center (TEC). The relative vertical accuracy of the LIDAR elevation measurements is a few centimeters. The area shown in Figure 8 covers approximately one square kilometer with 1 m post spacings.

The difference between the IFSAR DEM and the LIDAR DEM is illustrated in Figure 9 using a colormapped rendering. The color scale ranges from -2 m to +2 m. The correlation magnitude data were thresholded during interferometric processing at a value of 0.7 to produce a quality mask. This mask was applied to the difference image to exclude reduced quality (low correlation) measurements. As shown in Figure 9, this mask effectively excludes the trees and their shadows. A histogram of the differences is also shown in the Figure 6. The standard deviation of the differences is 29.9 cm. This corresponds to a point-to-point relative LE90 value of 69.5 cm.

Figure 10 shows an ortho-image mosaic of the Camp Roberts test site composed of 4 SAR magnitude images, 2 from pass GTM0211 and 2 from pass GTM0206. The images were ortho-rectified using the IFSAR derived

Figure 7: Interferogram corresponding to the SAR magnitude image show in Figure 5. The vertical ambiguity height (the height change corresponding to one light-to-dark phase fringe) is approximately 18 m. Note the clearly visible trails and dry stream bed.

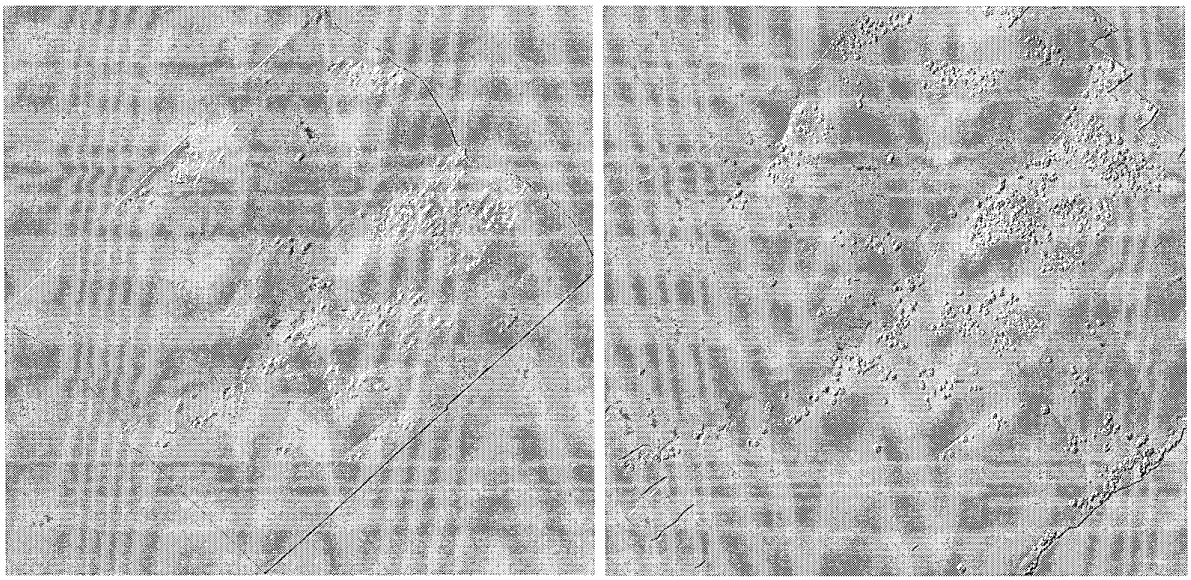

Figure 8: Shaded surface renderings comparing the long-baseline IFSAR elevation data (left) and LIDAR elevation data (right).

elevation data. The ortho-image is shown in a north-up UTM map projection with 1 m pixel spacing. The area corresponding to Figures 5 and 7 is visible in the upper portion of the ortho-image mosaic.

6. SUMMARY AND CONCLUSIONS

Large-baseline IFSAR systems have been suggested as a possible source for the production of precision elevation data with post spacings of 1 m and random errors less than 1 m. ERIM International has developed an airborne X-band IFSAR system capable of collecting single-pass interferometric SAR data with cross-track baselines of 7.5 m, 15 m, and 30 m. Data processing using interferometric techniques developed at ERIM International has produced elevation data with 1 m post spacings from 1-foot resolution SAR imagery. The resulting IFSAR elevation data have been compared with highly accurate LIDAR elevation data in order to estimate the accuracy of the IFSAR elevation measurements. The standard deviation of the differences between the IFSAR elevations and the LIDAR elevations is 29.9 cm. This corresponds to a point-to-point relative LE90 value of 69.5 cm, for points separated by distances up to approximately 1 km.

We believe these initial results demonstrate the significant utility of a large baseline IFSAR system for precision terrain mapping. The IFSAR-derived digital elevation data and ortho-image data can be provided to interested end-users upon request.

The support and encouragement of this work from Major Earl White of the US Air Force and Dr. William Jeffrey of the DARPA/TTO are gratefully acknowledged.

REFERENCES

[1] G. F. Adams, D. A. Ausherman, S. L. Crippen, G. T. Sos, B. P. Williams, "The ERIM Interferometric SAR: IFSARE" in *IEEE National Radar Conference*, Ann Arbor, Michigan, pp. 249-254, May 13-16, 1996.

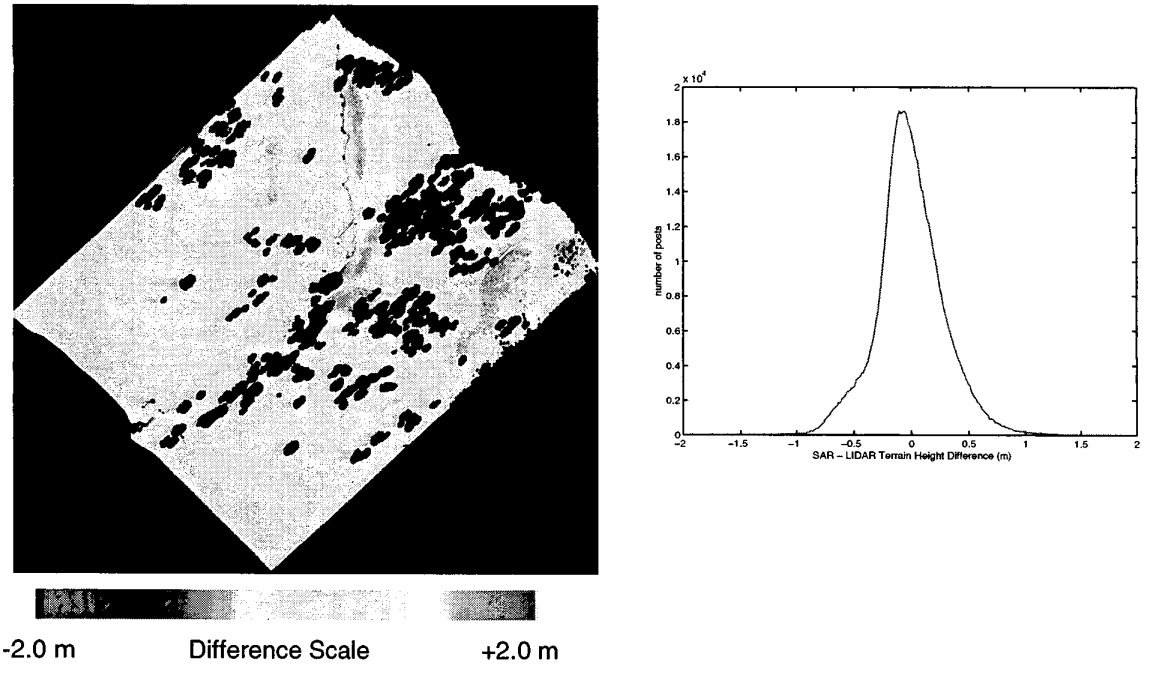

Figure 9: Differences between IFSAR elevation and LIDAR elevation rendered in color (left) and a histogram of the differences (right). The black areas are "no measurement" areas where the correlation level dropped below the 0.7 correlation threshold.

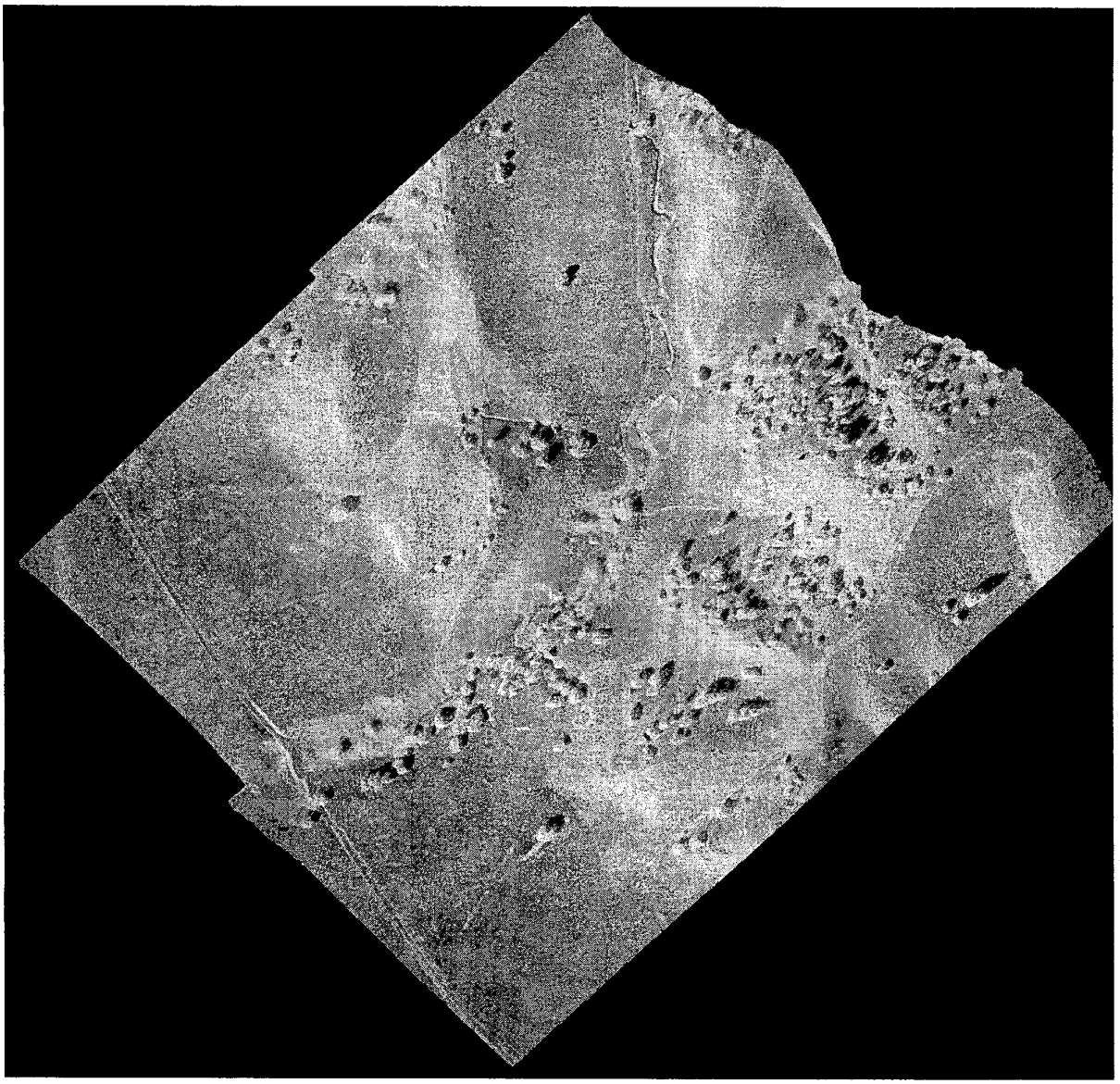

Figure 10: Ortho-image mosaic of the Camp Roberts test site composed of four SAR magnitude images, ortho-rectified using the IFSAR derived elevation data. The ortho-image is shown in a north-up UTM map projection with 1 m pixel spacing. The area corresponding to Figures 5 and 7 is visible in the upper portion of the ortho-image mosaic.

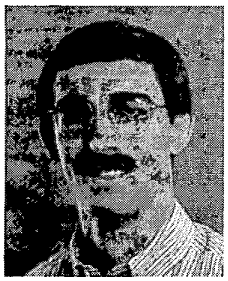

Neil Carender (M'84) received the B.E.E. degree with high honors from General Motors Institute in 1984, and the M.S. and Ph.D. degrees in electrical and computer engineering from Carnegie Mellon University in 1989 and 1991, respectively.

From 1991 to 1994, he was with the Digital Processing Laboratory at the Information Systems Division of Harris Corporation, where he was involved with the design and development of software and algorithms for autonomous image registration. In 1994, he joined Veridian ERIM International (formerly the Environmental Research Institute of Michigan), where he has performed research on a variety of topics related to topographic mapping using synthetic aperture radar.

J. Craig Dwyer received the B.S. degree in mathematics and the MS degree in physics, both from the University of Michigan in 1967 and 1969, respectively.

He is currently a Chief Engineer in the Sensor Development and Applications Group of Veridian ERIM International (formerly the Environmental Research Institute of Michigan), which he joined in 1973. Since 1979 he has done research and/or managed programs in SAR interferometry and many other applications of SAR phase information. Prior to that he worked on optical processing of SAR data.

From 1969 to 1973, he worked for Conductron Corporation, McDonnell Douglas Electronics Co. and Harris Electro-Optics Center, where he did research on a variety of coherent optical processing and holography topics.

He is a member of the Optical Society of America.

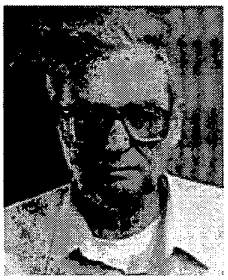

James Abshier received a B.S.E.E. degree from the University of Michigan in 1965 and an M.S.E.E. degree from Wayne State University in 1972. From 1965 until 1981 he was with Bendix Research Laboratories where he participated in the development of a variety of analytical photogrammetric systems. In 1981 he joined Veridian ERIM International where he has been involved in metric exploitation of SAR. His work with SAR includes the development of mathematical models for topographic mapping, target geolocation and error analysis.

Eric Cowen received the B.S.E.E. degree from the University of Michigan, Ann Arbor in 1980. He has been employed by Veridian ERIM International since 1980, where he has been involved in the performance analysis and system design of several fine resolution synthetic aperture radar sensors.

Brent Howlett received a B. S. degree in Math-Physics/Secondary Education from SUNY at Fredonia in 1978. He received a M. S. degree in Physics from Arizona State University in 1981.

He worked at Goodyear Aerospace Corporation, Arizona Division, from 1980 to 1985, on Synthetic Aperture Radar (SAR) image interpretation algorithms and systems. He has been employed by Veridian-ERIM International, in Ann Arbor, MI since 1985, working on SAR image information extraction algorithms.